Toward Reliable Synthesis of Radiotracers for Positron Emission Tomography in PDMS Microfluidic Chips: Study and Optimization of the [^{18}F]Fluoride Drying Process

W.-Y. Tseng, J. S. Cho, X. Ma, A. Kunihiro, A. Chatziioannou and R. M. van Dam

Crump Institute for Molecular Imaging and Department of Molecular & Medical Pharmacology, UCLA School of Medicine, 570 Westwood Plaza, Los Angeles, CA, 90095

ABSTRACT

Positron Emission Tomography (PET) depends on the reliable synthesis of tracers labeled with radioisotopes such as fluorine-18 (F-18). Microfluidic systems are well-suited for the production of these tracers due to their ability to manipulate nanoliter to microliter volumes with high precision. Integration of the multi-step synthesis of tracers in a single chip has been demonstrated in devices fabricated from polydimethylsiloxane (PDMS), however, frequent device failures and high loss of radioactivity during synthesis have limited the progress of this technology. To identify the source of these problems, we are breaking down the entire process and investigating each step in detail, beginning with the evaporation step. A dedicated evaporation chip was designed and fabricated. Using a recently-developed radioactivity imaging system based on the detection of Cerenkov radiation, we have measured qualitatively the distribution of radioactivity in the chip at various points during the evaporative drying process. Using these data, we have optimized the chip and the drying process to achieve reliable operation with low loss of radioactivity

Keywords: Positron Emission Tomography (PET), Microfluidics, Cerenkov radiation, Radiochemical synthesis, Fluorine-18

1. INTRODUCTION

Positron Emission Tomography (PET) is a quantitative *in vivo* imaging tool for basic biomedical research and clinical studies, with extremely high sensitivity and molecular specificity to targets and pathways. PET depends on the reliable synthesis of tracers labeled with radioisotopes such as fluorine-18 (F-18). Today, tracers are produced in a centralized manner due to the high cost of equipment, infrastructure, and personnel required. However, this centralized model cannot provide diverse probes (aside from 2-deoxy-2-[^{18}F]fluoro-D-glucose ([^{18}F]FDG)) at reasonable cost. Microfluidic systems, having numerous advantages for tracer synthesis [1] , could enable the creation of a decentralized production model, making the development and use of diverse probes more accessible.

The preparation of [^{18}F]FDG is shown in Figure 1. It begins with the critical step of removing water from the [^{18}F]fluoride produced in the cyclotron. Generally, this is achieved by evaporation and azeotropic distillation with acetonitrile. After drying, tracers including [^{18}F]FDG are typically produced by a fluorination reaction in an anhydrous solvent, followed by a deprotection step. The final product is collected for purification and quality control.

Microfluidic systems have shown great promise to produce PET tracers labeled with F-18 due to their ability to manipulate nanoliter to microliter volumes with high precision [3]. Proof-of-concept demonstrations using PDMS microfluidic systems have shown that not only reactions, but all processes of the synthesis, can be integrated into a single chip [4][5]. However, previous studies have postulated incompatibilities of PDMS with ^{18}F-radiosyntheses, owing to frequent observations of device failures and F-18 loss. Poor understanding of these issues has limited further progress in this technology.

Recently we developed a novel quantitative radioactivity imaging system, based on the detection of Cerenkov radiation [6] that can provide insights into the detailed operation of microfluidic devices during

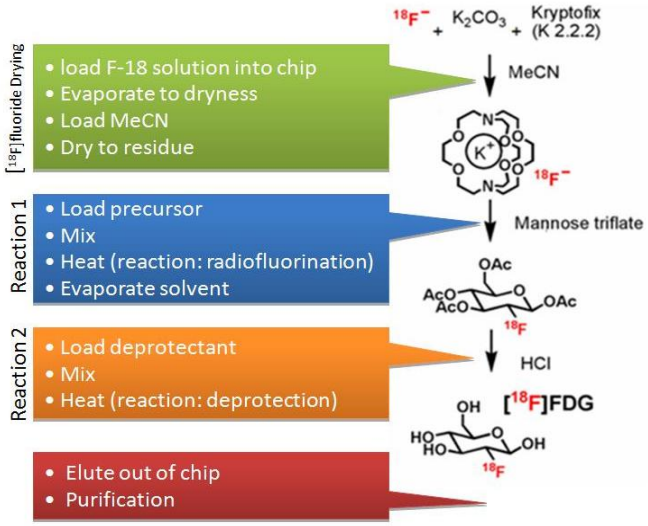

Figure 1: [^{18}F]FDG synthesis. (Left) Unit operations carried out in PDMS radiosynthesis chips. (Right) Chemical steps. After drying of [^{18}F]fluoride solution, mannose triflate is fluorinated to produce the intermediate [^{18}F]FTAG, which is then hydrolyzed with HCl to form [^{18}F]FDG.

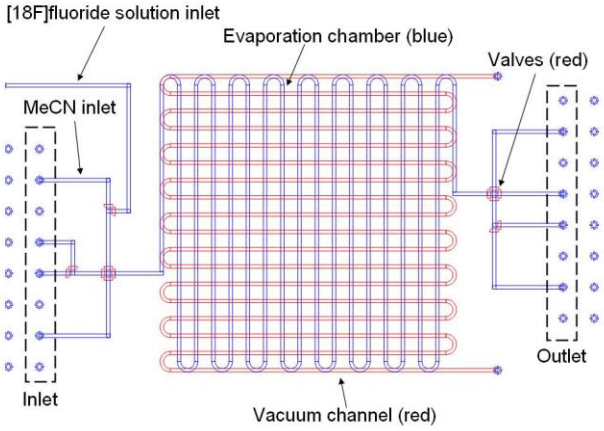

Figure 2: Design of PDMS evaporation chip. Fluid inlets and outlets and the evaporation chamber with volume 3.3µL are located in the fluid layer. The valve control channels and the vacuum channel are in the control layer.

radiotracer production. We are applying this tool and other techniques to investigate the PDMS chip approach, with the aim of uncovering the source of problems and ultimately converting this into a reliable platform for ^{18}F-radiosynthesis. In this paper, we study and optimize the [^{18}F]fluoride drying process, the first step of nearly all radiosyntheses involving F-18.

2. MATERIALS AND METHODS

2.1 Microfluidic chip design and fabrication

We have designed a dedicated, multi-layer PDMS chip to study drying of [^{18}F]fluoride by evaporation. The layout of the chip is shown in Figure 2. This chip includes three layers: PDMS fluid layer, PDMS control layer and glass substrate layer. The fluid layer (blue channels) contains reagent inlets and outlet and the serpentine evaporation chamber in which the [^{18}F]fluoride is loaded and dried. The control layer (red channels) includes the microvalve control channels and the serpentine vacuum channel. The states of the valves control the flow path of the reagents. The vacuum channels are perpendicular to and under the fluid channel (Figure 3). During the evaporation, the solvent is converted to the gas phase and permeates across the ~20 µm PDMS film where it is removed by the vacuum channel. The use of vacuum enhances the rate of evaporation of solvent during the drying step compared to chips without such a channel. Each chip was thoroughly tested and the burst pressure of its valves measured prior to use.

2.2 Reagents

Anhydrous acetonitrile (MeCN), Kryptofix 2.2.2, and potassium carbonate (K_2CO_3) were purchased from Sigma-Aldrich. No-carrier-added [^{18}F]fluoride ion, obtained from the UCLA Cyclotron and Radiochemistry Center, was produced in an RDS-112 cyclotron (Siemens). To prepare the [^{18}F]fluoride solution for evaporative drying, aqueous

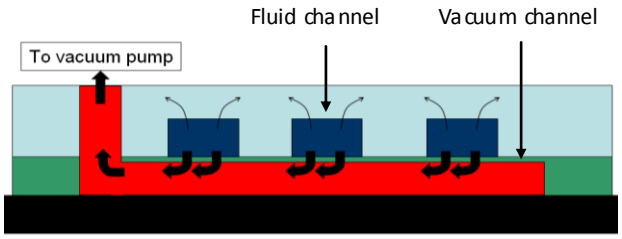

Figure 3: Mechanism of solvent evaporation from the evaporation chamber. Some vapor permeates into the PDMS matrix (thin arrows), but the highest flux (thick arrows) is through the thin PDMS membrane above the vacuum channel. Vacuum rapidly eliminates the vapor from the chip to maintain the pressure differential.

[^{18}F]fluoride ion was treated with K_2CO_3 and Kryptofix 2.2.2, a phase-transfer agent to a final concentration of 2.53mM K_2CO_3, 5.06mM Kryptofix 2.2.2 in MeCN/water (80:20 v/v).

2.3 Cerenkov imaging system for radioactivity detection

The microfluidic chip was operated inside a light-tight box with a sensitive lens-coupled CCD camera as shown in Figure 4. The temperature of the chip was controlled using a closed-loop thermoelectric (Peltier) system. Cerenkov radiation is emitted when energetic positrons from the

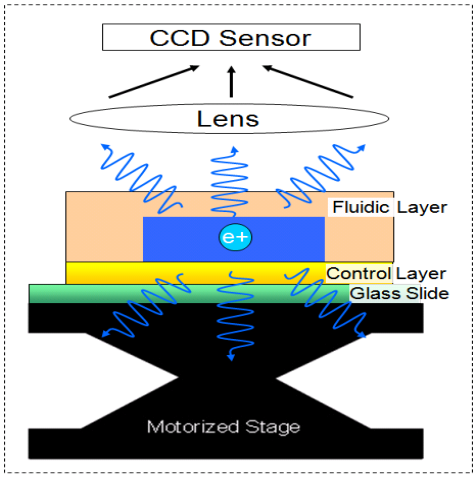

Figure 4: Schematic of Cerenkov imaging system

decay of F-18 travel through the surrounding medium (solvent, PDMS, glass) with a velocity greater than that of light in that material. This faint blue light is detected by the CCD camera, with intensity proportional to the radioactivity from a given location [6].

Multiple Cerenkov images were taken during the evaporation process, providing a measure of the radioactivity distribution and quantity within the chip at different time points such as after loading, after evaporation and after elution. To obtain sufficient signal, acquisition

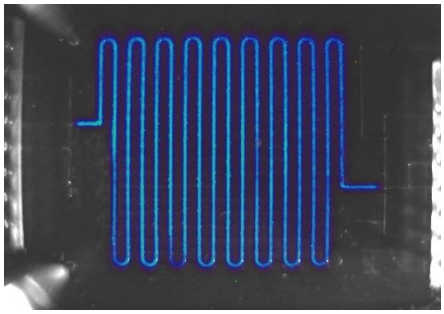

Figure 5: Example processed image of channel filled with F-18 solution (false color).

times were typically 5 minutes. Captured images were processed by dark current correction, flat field correction and decay correction to enable quantification of the amount of radioactivity inside regions of interest in the image. The image from Figure 5 is a typical processed image after loading of [^{18}F]fluoride solution into the microfluidic chip, just prior to evaporation.

2.4 Drying experiments

A 500µL aliquot of [^{18}F]fluoride solution, sufficient for multiple experiments, was prepared and loaded into a small V-vial. A portion of the resulting [^{18}F]fluoride solution was loaded via tubing into the evaporation chamber of the chip, filling it completely. After closing valves at the ends, liquid remaining in the channels outside the evaporation chamber was flushed out. This step can reduce camera noise, and make it easy to detect if valve leaks occur during evaporation. A Cerenkov image was taken to determine the initial quantity of radioactivity loaded in the chip.

To perform evaporation of solvent from the [^{18}F]fluoride solution, the chip was heated to 105°C and held at this temperature until all liquid disappeared. During this period a small LED light was illuminated inside the box, allowing the same CCD camera to monitor the whole evaporation process in bright-field. After elimination of the solvent, the system was then cooled to room temperature and a second Cerenkov image was obtained to determine the remaining radioactivity. The chip was cleaned by flushing the channel with large volumes of MeCN and water to permit multiple experiments in the same day.

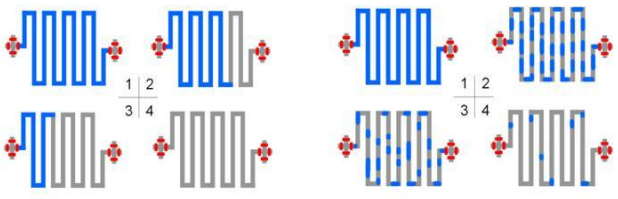

Figure 6: Schematic evolution of liquid during (left) directional and (right) burst evaporation patterns. Liquid in the evaporation chamber is represented in blue; air in gray.

3. RESULTS AND DISCUSSION

3.1 Optimization of operating temperature can avoid valve leaks

The "burst pressure" of a valve is the maximum pressure that a valve can withstand without any leakage. Empirical tests of on-chip microvalves found the burst pressure is typically 40 psig. We chose 105°C as the operation temperature in our studies at which MeCN vapor pressure is 28 psig (giving 30% engineering safety margin). It should be noted that previous work in PDMS radiosynthesis chips used temperatures up to 140°C which generates high vapor pressures (70 psig for MeCN). It therefore is likely that previous experiments suffered from valve leakage issues including cross-contamination of reagents or loss of radioactivity from the chip.

3.2 Two patterns of evaporation progression

Two different evaporation patterns were observed, which we refer to as "burst" and "directional" (Figure 6). The patterns have qualitatively different progression as observed in bright-field. "Directional" evaporation occurs when an initial bubble exists in the channel and grows as the liquid becomes progressively more concentrated as its volume shrinks. The result is that all the [^{18}F]fluoride residue and associated salts become concentrated at one (or two) ends of the evaporation chamber. "Burst" evaporation generally occurs with no initial air bubbles. Evaporation of solvent leads to deformation of the PDMS and partial collapse of the channel. Eventually, we hypothesize, a sudden release of elastic energy and nucleation of vapor bubbles causes the channel to return to its original shape, fragmenting the remaining liquid into relatively uniform liquid slugs. Each slug rapidly shrinks by evaporation leaving [^{18}F]fluoride residue "spots" uniformly throughout the channel.

3.3 Channel clogging / valve sticking likely caused by salt residue

The "directional" evaporation pattern was correlated with chip failures. Cerenkov images after evaporation showed that chips undergoing directional evaporation had radioactivity concentrated at inlets or outlets of the evaporation chamber while burst evaporation resulted in activity distributed evenly along the channel (Figure 7). Examination by optical microscopy after directional evaporations confirmed that regions of high radioactivity were correlated with the locations of clogged channels and/or permanently-stuck valves. In contrast, no chips that underwent burst evaporation had these failures. Clogging is probably due to the accumulation of salts/residue in a very short section of channel. This suggests a burst-like evaporation pattern would be favorable for reliable operation.

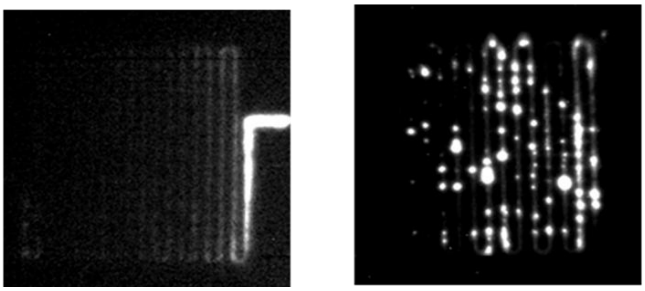

Figure 7: Radioactivity images after evaporation. Bright areas indicate higher radioactivity. (Left) Directional evaporation pattern shows most [^{18}F]fluoride accumulated at one end of the channel; (Right) Burst evaporation pattern result shows more uniform distribution of dry [^{18}F]fluoride.

3.4 Minimization of radioactivity loss during evaporation

After the evaporation step, we found the loss of radioactivity to be < 10% compared to the activity before the evaporation. Higher loss of radioactivity was observed in chips if heating was continued after evaporation of solvent was complete (Figure 8). Radioactivity loss increases with heating time. As a control, measurements at room temperature show negligible loss of radioactivity over time, confirming temperature dependence of this process. Taken together, these results suggest how 90% loss was previously observed [1] and suggest a strategy to avoid the loss. We suspect the loss originates from a reaction between F-18 and PDMS that forms volatile compounds (leading to loss) as well as integration of F-18 into PDMS matrix (leading to unflushable residue, data not shown). Since directional evaporations typically require significantly longer heating times, these data suggest a second reason for preference of the burst evaporation pattern.

4. CONCLUSION

In a short time, the Cerenkov imaging system has helped pinpoint several sources of chip failure that could have contributed to reliability issues in earlier studies. By designing our chip and process to avoid these conditions, [^{18}F]fluoride can reliably be dried in a PDMS chip without significant loss. Studies are underway to assess and optimize the dryness of F-18 using radiofluorination reactions as a benchmark. Also, we are in the process of designing new PDMS radiosynthesizer chips to continue our study of the remaining synthesis steps.

5. ACKNOWLEDGMENTS

This work was supported in part by the Industry-University Cooperative Research Program and Sofie Biosciences, Inc. ,(UC Discovery Grant number bio08-129095), and a grant from the National Institutes of Health (SAIRP NIH-NCI 2U24 CA092865). We would like to thank Prof. Nagichettiar Satyamurthy and the staff of the UCLA Cyclotron and Radiochemistry Center for providing

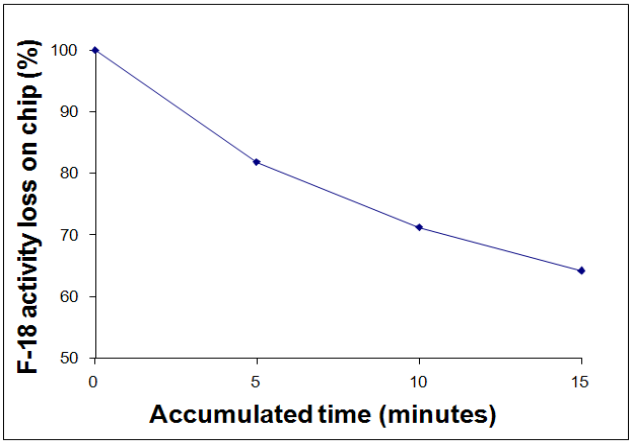

Figure 8. Radioactivity is lost from the evaporation chamber if heating is continuing after evaporation of solvent is complete. The first image, taken after evaporation at 25°C, is normalized to 100%. Subsequent images are taken after heating the chip to 105°C and cooling to 25°C.

.

[^{18}F]fluoride, and Prof. Kwang-Fu Clifton Shen and his lab for use of a mini-cell and analytical equipment.

REFERENCES

[1] A.M. Elizarov, "Microreactors for radiopharmaceutical synthesis," *Lab on a Chip*, vol. 9, 2009, pp. 1326-1333.

[2] H. Audrain, "Positron Emission Tomography (PET) and Microfluidic Devices: A Breakthrough on the Microscale?," *Angewandte Chemie International Edition*, vol. 46, 2007, pp. 1772-1775.

[3] P.W. Miller, "Radiolabelling with short-lived PET (positron emission tomography) isotopes using microfluidic reactors," *Journal of Chemical Technology & Biotechnology*, vol. 84, 2009, pp. 309-315.

[4] C. Lee, G. Sui, A. Elizarov, C. Shu, Y. Shin, A. Dooley, J. Huang, A. Daridon, P. Wyatt, D. Stout, H. Kolb, O. Witte, N. Satyamurthy, J. Heath, M. Phelps, S. Quake, and H. Tseng, "Multistep Synthesis of a Radiolabeled Imaging Probe Using Integrated Microfluidics," *Science*, vol. 310, 2005, pp. 1793-1796.

[5] A.M. Elizarov, R.M. van Dam, Y.S. Shin, H.C. Kolb, H.C. Padgett, D. Stout, J. Shu, J. Huang, A. Daridon, and J.R. Heath, "Design and Optimization of Coin-Shaped Microreactor Chips for PET Radiopharmaceutical Synthesis," *J Nucl Med*, vol. 51, Feb. 2010, pp. 282-287.

[6] J.S. Cho, R. Taschereau, S. Olma, K. Liu, Y. Chen, C.K. Shen, R.M. van Dam, and A.F. Chatziioannou, "Cerenkov radiation imaging as a method for quantitative measurements of beta particles in a microfluidic chip," *Physics in Medicine and Biology*, vol. 54, 2009, pp. 6757-6771.